

This is a self-archived version of an original article. This version may differ from the original in pagination and typographic details.

Author(s): Riuttamäki, Saara; Laszkó, Gergely; Madarász, Ádam; Földes, Tamás; Pápai, Imre; Bannykh, Anton; Pihko, Petri M.

Title: Carboxylate catalyzed isomerization of β,γ -unsaturated N-acetylcysteamine thioesters

Year: 2022

Version: Published version

Copyright: © 2022 The Authors.

Rights: CC BY 4.0

Rights url: <https://creativecommons.org/licenses/by/4.0/>

Please cite the original version:

Riuttamäki, S., Laszkó, G., Madarász, Á., Földes, T., Pápai, I., Bannykh, A., & Pihko, P. M. (2022). Carboxylate catalyzed isomerization of β,γ -unsaturated N-acetylcysteamine thioesters. *Chemistry : A European Journal*, 28(45), Article e202201030. <https://doi.org/10.1002/chem.202201030>

Carboxylate Catalyzed Isomerization of β,γ -Unsaturated *N*-Acetylcysteamine Thioesters**

Saara Riuttamäki,^[a] Gergely Laczkó,^[b] Ádám Madarász,^[b] Tamás Földes,^[b] Imre Pápai,^{*,[b]} Anton Bannykh,^[a] and Petri M. Pihko^{*,[a]}

Abstract: We demonstrate herein the capacity of simple carboxylate salts – tetramethylammonium and tetramethylguanidinium pivalate – to act as catalysts in the isomerization of β,γ -unsaturated thioesters to α,β -unsaturated thioesters. The carboxylate catalysts gave reaction rates comparable to those obtained with DBU, but with fewer side

reactions. The reaction exhibits a normal secondary kinetic isotope effect ($k_{1H}/k_{1D}=1.065\pm 0.026$) with a β,γ -deuterated substrate. Computational analysis of the mechanism provides a similar value ($k_{1H}/k_{1D}=1.05$) with a mechanism where γ -reprotonation of the enolate intermediate is rate determining.

Introduction

In the laboratory, enolizations of esters, thioesters and ketones are typically carried out with strong, non-nucleophilic bases such as hindered alkali amide bases, for example lithium diisopropylamide (LDA) or potassium hexamethyldisilazide (KHMDs).^[1] In contrast, in vivo, enzymatic enolization of thioesters or ketones proceeds readily with mild carboxylate ions as the catalytic bases. Enzymes such as citrate synthase^[2,3] and ketosteroid isomerase (KSI)^[4,5] use the carboxylate side chain of aspartate as the general base, and aspartate or glutamate carboxylates are the general bases in the crotonase superfamily^[6] of enzymes. As an example, Δ^3,Δ^2 -enoyl-CoA-isomerases (ECIs) catalyze the isomerization of β,γ -unsaturated coenzyme A (CoA) thioesters **3** to their α,β -unsaturated isomers **4** (Scheme 1).^[7,8] The isomerization is a key step in fatty acid degradation and these enzymes are present in both mitochondria and peroxisomal cell organelles of eukaryotes. In the active site of the human mitochondrial Δ^3,Δ^2 -enoyl-CoA-isomerase (hmECI), the catalytic base is a glutamate residue (Glu136,

Scheme 1).^[9] The γ -carbon of the substrate is protonated by Glu136 (Scheme 1).

The general bases at the active sites of enolizing enzymes are not sufficiently basic to deprotonate α -protons of carbonyl compounds on their own.^[10] The α -C–H groups of thioesters and ketones have pK_a s in the range of 18–21,^[10] whereas the carboxylate bases have pK_{aH} 's of only ca. 4.8 (Asp 3.9 and Glu 4.25 in water).^[11] The high rates of the enzymatic enolization reactions have been rationalized by the additional assistance of the oxyanion hole of the enzymes that either stabilizes the enolate intermediate by hydrogen bonding, or *O*-protonates the enolate giving an enol.^[10] However, more recent studies with KSI^[12] involving careful site-directed mutagenesis studies at the oxyanion hole, have provided evidence that the oxyanion hole of KSI provides only moderate contribution to increasing the catalytic rate (by ca. 10^3 -fold), suggesting that the hydrophobic binding cavity and the general base catalysis alone can provide significantly enhanced rates (10^3 -fold) compared to reactions in water.

These results suggest that in a hydrophobic, aprotic environment, carboxylates might be more powerful catalytic bases than their aqueous pK_a s would suggest. In a singular example, Ooi and co-workers have recently demonstrated that chiral phosphonium carboxylates can be used for catalytic Mannich reaction of azlactones in THF.^[13] Surprisingly, carboxylates are very rarely used as base catalysts for organic synthesis^[14] outside of the realm of enzymes.

Herein we show that tetramethylammonium pivalate (TMAP), a carboxylate salt, rapidly isomerizes β,γ -unsaturated thioesters to their α,β -unsaturated isomers in MeCN via a mechanism that involves a rate-determining protonation of the intermediate enolate.

Results and discussion

To mimic the reaction mechanism of ECI, we used a biomimetic system with *N*-acetylcysteamine (NAC) thioesters as substrates.

[a] S. Riuttamäki, A. Bannykh, Prof. Dr. P. M. Pihko
Department of Chemistry
University of Jyväskylä
P.O. Box 35, 40014, Jyväskylä (Finland)
E-mail: petri.m.pihko@jyu.fi

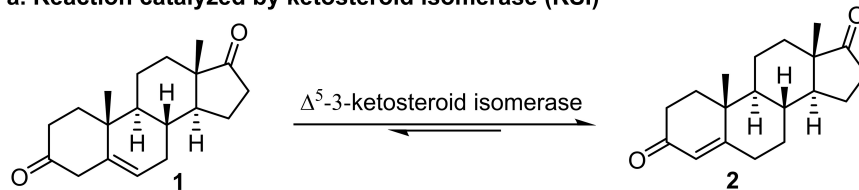
[b] G. Laczkó, Dr. Á. Madarász, Dr. T. Földes, Dr. I. Pápai
Institute of Organic Chemistry
Research Centre for Natural Sciences
Magyar tudósok körútja 2, 1117, Budapest (Hungary)
E-mail: papai.imre@ttk.hu

[**] A previous version of this manuscript has been deposited on a preprint server (<https://doi.org/10.26434/chemrxiv-2022-cvmqf>).

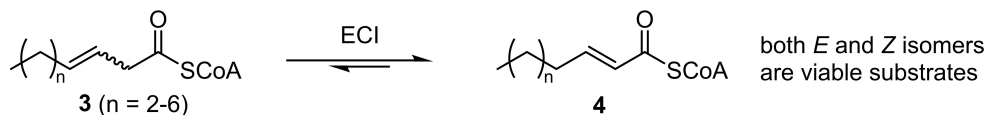
Supporting information for this article is available on the WWW under <https://doi.org/10.1002/chem.202201030>

© 2022 The Authors. Chemistry - A European Journal published by Wiley-VCH GmbH. This is an open access article under the terms of the Creative Commons Attribution Non-Commercial NoDerivs License, which permits use and distribution in any medium, provided the original work is properly cited, the use is non-commercial and no modifications or adaptations are made.

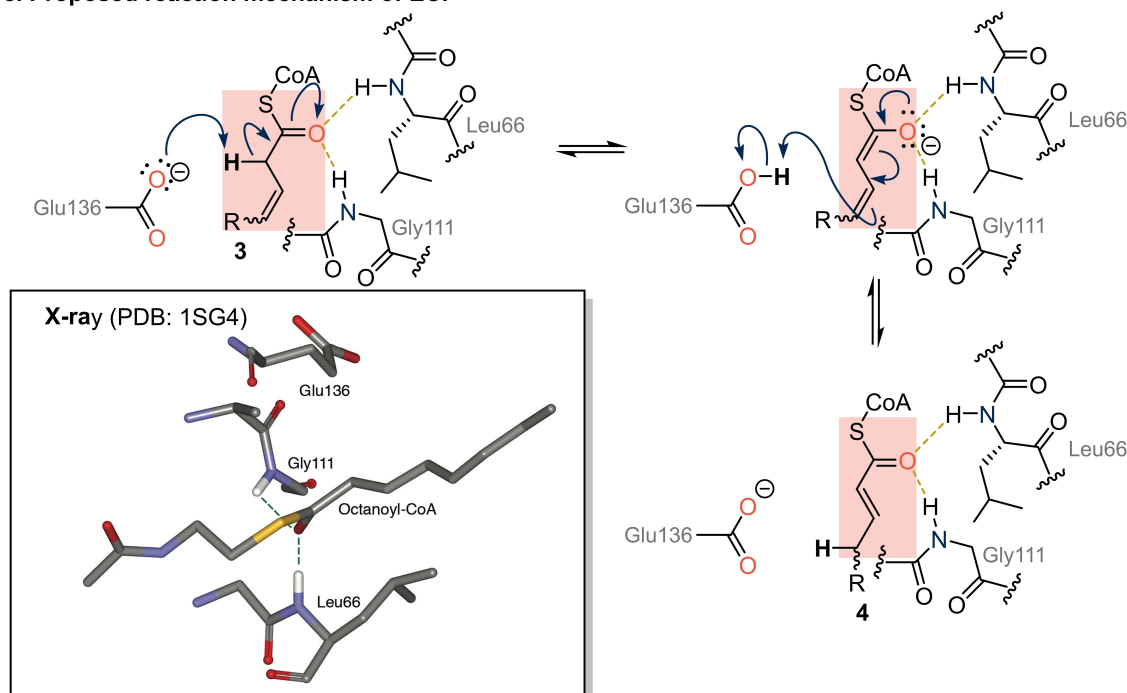
a. Reaction catalyzed by ketosteroid isomerase (KSI)



b. Isomerization catalyzed by enoyl isomerase (ECI)



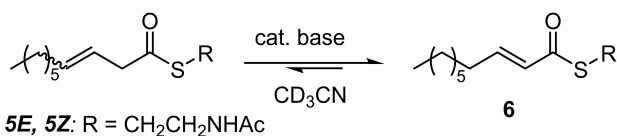
c. Proposed reaction mechanism of ECI



Scheme 1. Isomerization reactions catalysed by a) ketosteroid isomerase (KSI), b) enoyl-CoA isomerase (ECI) and c) proposed reaction mechanism for ECI-catalyzed isomerization of β,γ -unsaturated CoA-thioesters. The X-ray structure of ECI complexed with the unreactive substrate analogue, octanoyl-CoA is shown in inset. (PDB code: 1SG4).

In lieu of the glutamate base, we used tetramethylammonium pivalate (TMAP) or tetramethylguanidinium pivalate (TMGP). For comparison, non-ionic bases DBU and Et_3N were also used. The reaction progress was monitored by ^1H NMR (Scheme 2). Both *Z*- and *E*-isomers of β,γ -unsaturated NAC-thioesters were synthesised.

Thioesters **5E** and **5Z** were synthesised in two and four steps, with overall yields of 13% and 17% respectively

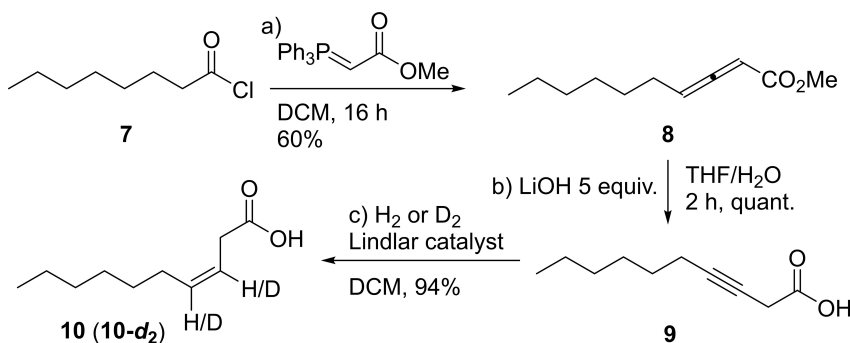


Scheme 2. Catalytic isomerization of unsaturated NAC thioesters.

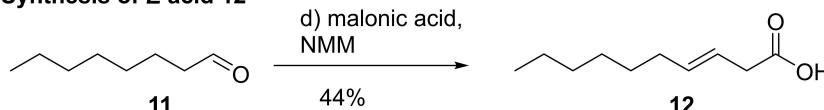
(Scheme 3).^[15,16] The deuterated variant **5Z-d₂** was synthesized using the same route, using D_2 in the Lindlar reduction step (Scheme 3). The β,γ -unsaturated carboxylic acids and their derivatives were sensitive to premature isomerization, requiring the use of very mild conditions for the final thioester formation step (Table 1).

Standard coupling conditions (DCC in DCM) led to concomitant isomerization to the α,β -unsaturated isomer (Table 1, entry 1). With EDC·HCl (entry 2) the product was almost completely isomerized. While diisopropylcarbodiimide (DIC) caused no isomerization, the side product diisopropylurea (DIU) could not be separated from the product (entries 3 and 4). Finally, acceptable levels of isomerization were obtained using DCC in acetonitrile, as the resulting dicyclohexylurea is only sparingly soluble in acetonitrile, and a maximum of 3.5% isomerization was observed (entry 6).

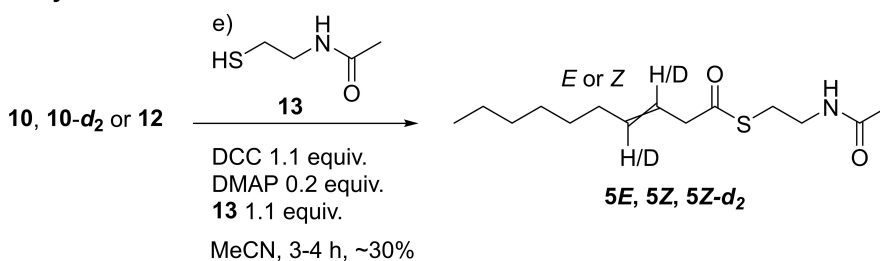
A. Synthesis of Z acid 10



B. Synthesis of E acid 12



C. Synthesis of NAC thioesters



Scheme 3. Synthesis of NAC thioesters.

Table 1. Optimization of the thioesterification of β,γ -unsaturated carboxylic acids.

Entry	Coupling reagent	Solvent	Reaction time [h]	Product	Yield [%]	Premature isomerization [%]
1	DCC	DCM	2.5	5Z	75*	16
2	EDC-HCl	DCM	2	5Z	18	70
3	DIC	DCM	2	5Z	60 ^[a]	0
4	DIC	MeCN	1.5	5Z	56 ^[a]	0
5	DCC	MeCN	3	5Z	36	3.5
6	DCC	MeCN	3	5E	28	0
7	DCC	MeCN	3	5Z- d_2	64	< 3%

[a] Product and large amounts of DCU or DIU

The DCC/MeCN method was also used for the preparation of thioesters **5E** and **5Z- d_2** , with 28 and 64% yields, respectively (Table 1).

For the isomerization experiments, we initially screened Et_3N as the base, but the reaction rates were very low, with **5E** taking 50 days to reach equilibrium (30 days with **5Z**). We then turned to stronger bases. The results of these base-catalyzed isomerization reactions are summarized in Figure 1 and Table 2. As shown in Table 2, the rate of isomerization was faster with

Table 2. Rates of isomerization with different catalysts

Entry	Substrate	Catalyst	Rate [mmol L ⁻¹ s ⁻¹]	Reaction time [h]
1	5E	DBU	1.23 ± 0.05	2
2	5E	TMAP	0.15 ± 0.003	16
3	5E	TMGP	0.04 ± 0.02	16
4	5Z	DBU	10.5 ± 0.49	0.35
5	5Z	TMAP	5.47 ± 1.12	0.35
6	5Z	TMGP	0.20 ± 0.36	16

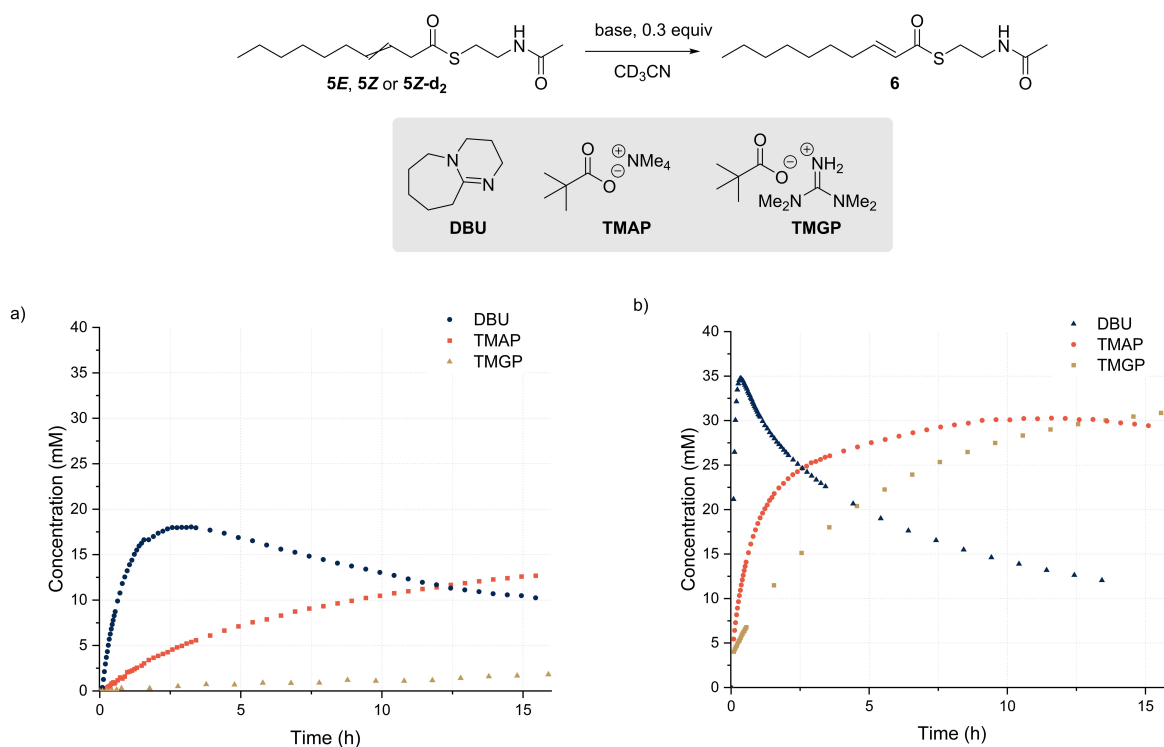


Figure 1. Isomerization of **5E** (left) and **5Z** (right) with DBU, TMAP and TMGP. Reaction conditions: 27 μmol of thioester in 600 μL of CD_3CN , 0.3 equiv. of TMAP, TMGP or DBU, dibenzyl ether as internal standard. The reactions were monitored by ^1H NMR (see the Supporting Information for details).

5Z compared to **5E** irrespective of the base used (Figure 1). With DBU, the initial rate is with the *Z* isomer almost tenfold compared to the rate with **5E**. However, DBU also leads to rapid product decomposition, complicating the rate measurement. With the carboxylate base catalyst, TMAP, **5Z** isomerizes >30 times faster than the **5E**, with significantly less product decomposition. The rate difference is less pronounced with TMGP, which is also less efficient as a catalyst compared to TMAP.

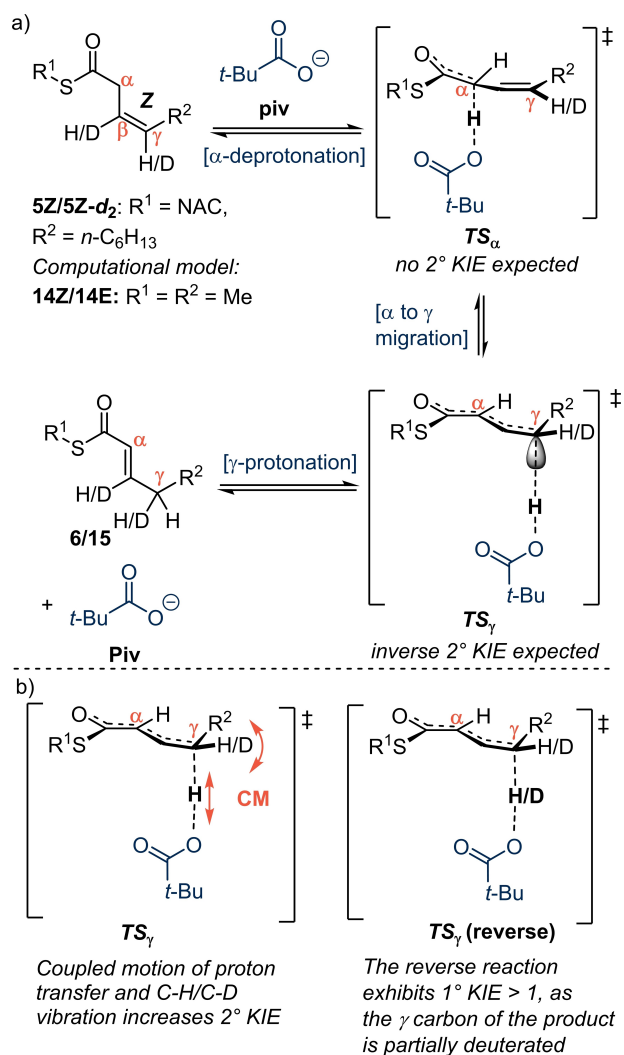
Leito and co-workers^[17,18,19,20] have measured and calculated $\text{p}K_{\text{a}}$ values for various acids and bases in non-aqueous media. According to their results, the $\text{p}K_{\text{a}}$ of acetate and DBU in acetonitrile are 23.8 and 24.3, respectively. These $\text{p}K_{\text{a}}$ s correlate nicely with our experimental results: with DBU the rate is higher than with TMAP with both **5E** and **5Z**, but the carboxylate base (TMAP) catalyses the reaction at a comparable rate (see Table 2, entries 1 vs. 2 and 4 vs. 5). The $\text{p}K_{\text{a}}$ values of these bases in water are, however, not reliable indicators of reactivity: the $\text{p}K_{\text{a}}$ of DBU is 11.9 and the $\text{p}K_{\text{a}}$ of the acetate ion is 4.8.^[21]

To investigate the reaction mechanism, we hypothesized that the reaction might take place via discrete proton transfer/migration events (Scheme 4), catalysed by the pivalate anion (**piv**) of TMAP and TMGP. The overall rate could be controlled by either the α -deprotonation, α -to- γ -migration, or γ -reprotonation steps (Scheme 4). If the last step contributed significantly to the reaction rate, the reaction might exhibit a secondary KIE if the γ -position is deuterated. To explore this possibility, we carried out a reaction progress kinetic study with quadruplicate measurements using **5Z** and 3,4-dideuterated **5Z-*d*₂** (see

Scheme 4) as substrates. To account for the reversibility of the reaction, the rates of the forward reaction (k_1) as well as the reverse reaction (k_{-1}) were determined from the data via COPASI simulations (see the Supporting Information). These data provided a KIE of $k_{1\text{H}}/k_{1\text{D}} = 1.065 \pm 0.026$ for the forward reaction and $k_{-1\text{H}}/k_{-1\text{D}} = 1.659 \pm 0.097$ for the reverse reaction.

While a normal KIE would be expected for the reverse reaction as it involves a C–H or C–D bond cleavage at the γ -carbon, the observed normal 2° KIE for the forward reaction does not appear to be consistent with the hybridization changes during the reaction. If the protonation of the γ -carbon of the enolate intermediate is rate-determining, an inverse 2° KIE would be expected based on sp^2 to sp^3 hybridization change (Scheme 4). Alternatively, a rate-determining α -deprotonation should result in a 2° KIE close to 1.00.

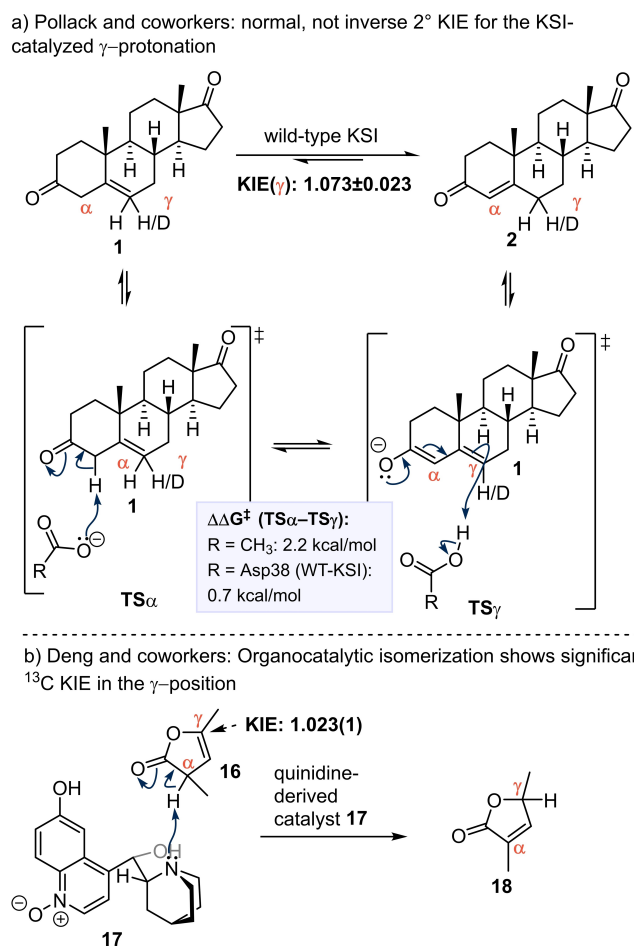
However, these seemingly abnormal 2° KIEs may also be a result of coupled motion (CM) or CM combined with hydrogen tunnelling (HT) (Scheme 4b). Pollack and coworkers have carried out a systematic study of the KIEs in a related isomerization reaction catalysed by KSI (Scheme 5) and determined the intrinsic KIEs for the key γ -protonation step.^[22] The experimental 2° KIE for the KSI-catalyzed γ -protonation step (1.073 ± 0.023) is very close to the KIE observed herein, and the slow acetate-catalyzed isomerization of **1** in solution also displayed a normal KIE (1.031 ± 0.010). Independently of the KIEs, free energy diagrams and rate constants for all individual steps have been determined for the KSI catalyzed reactions, and they show that the γ -protonation has a higher barrier than the α -deprotonation (the $\Delta\Delta G^\ddagger$ between TS_α and TS_γ is 0.7 kcal/mol for the reaction



Scheme 4. a) Simplified mechanism and the system examined computationally (14/15). The β -deuterium label of 5Z-d₂ has been omitted in the TS diagrams. b) Rationalization of the (ab)normal 2° KIE by the coupled motion (CM) hypothesis and explanation of the magnitude of the KIE of the reverse reaction.

catalysed by wild-type KSI and 2.2 kcal/mol for the acetate-catalyzed reaction).^[22,23] Finally, in another related isomerization reaction, catalysed by cinchona alkaloid organocatalyst 17, carbon isotope effects also indicated a rate-determining γ -protonation (KIE = 1.023, see Scheme 5).^[24,25]

Overall, the KIE studies are compatible with previously proposed mechanisms for the conjugate isomerization reactions via enolization involving rate-determining γ -protonation. To investigate the mechanism further and to compare computationally determined KIEs with the experimental values, we carried out DFT calculations for the isomerization of simplified model thioesters (14Z and 14E), using the pivalate anion (piv) as a base catalyst (Scheme 4; for computational details, see the Supporting Information).^[26] The computed free energy diagram and the structures of the relevant intermediates and transition states for the reaction with thioester 14Z are depicted in



Scheme 5. Previous KIE studies of conjugate isomerization reactions. In both cases, the γ -protonation step has the highest barrier.

Figures 2 and 3. The results obtained for thioester 14E are reported in the Supporting Information.

The isomerization of 14Z is initiated by the deprotonation of the CH₂ group at the α -position, which occurs via ts₁ with a fairly low barrier (15.9 kcal/mol). Facile rearrangement of intermediate int₁ via ts₂ gives intermediate int₂, which is preorganized for proton transfer to the γ -carbon of the enolate. The γ -protonation transition state ts₃ is predicted to be at 19.3 kcal/mol on the free energy scale, so it represents the rate-determining step of the isomerization. The energy difference between ts₃ and ts₁ is 3.4 kcal/mol, which is comparable to the experimentally determined difference (2.2 kcal/mol) between the α -deprotonation and γ -protonation transition states for the isomerization of 1 to 2 (see Scheme 5a).^[22,23] Importantly, the calculated isotope effects ($k_{1H}/k_{1D} = 1.05$ for the forward reaction and $k_{1H}/k_{1D} = 1.67$ for the reverse reaction, see the Supporting Information) are in excellent agreement with the experimentally obtained values. For the isomerization of 14E, computations predict similar mechanism with a slightly higher barrier (21.6 kcal/mol; see the Supporting Information). The higher barrier with 14E compared to 14Z also agrees with experimental observations.

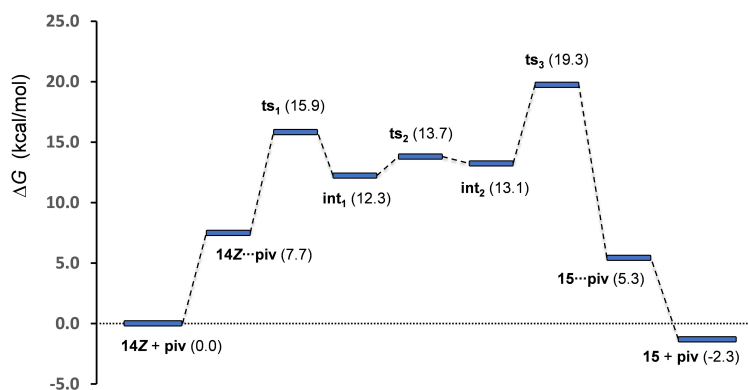


Figure 2. Gibbs free profile computed for the isomerization of **14Z** catalyzed by **piv**. Relative stabilities are shown in parentheses (in kcal/mol; with respect to the reactant state **14Z + piv**).

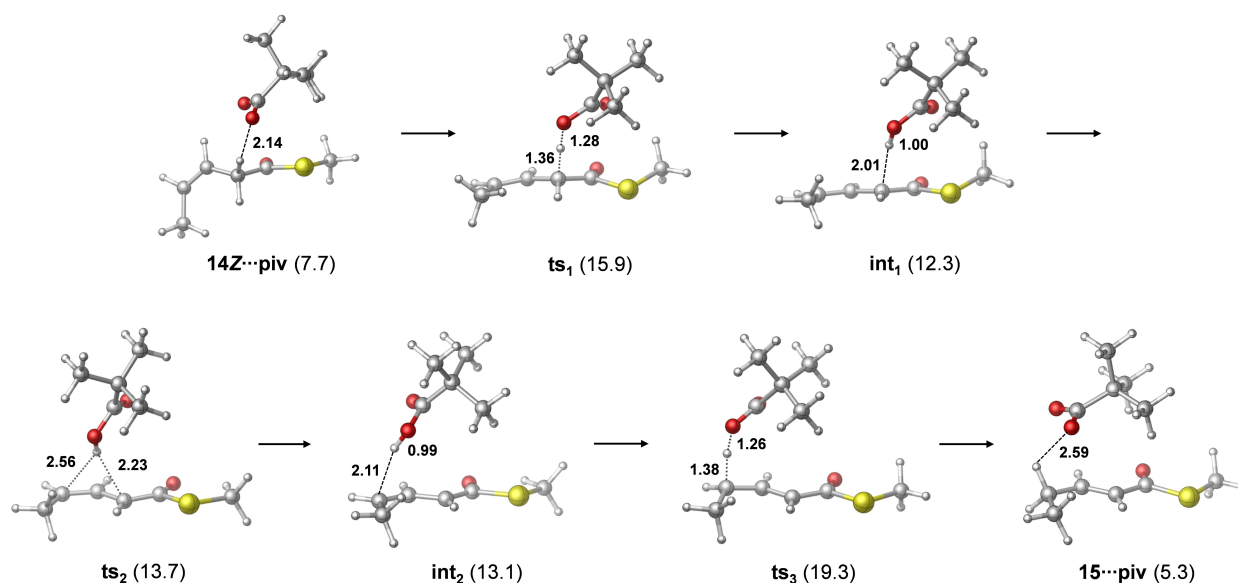


Figure 3. Optimized structures of species identified computationally for the isomerization of **14Z** catalyzed by **piv**. Relative stabilities are shown in parentheses (in kcal/mol; with respect to the reactant state **14Z + piv**). Selected bond distances are given in Å.

In addition to pivalate as a base, isomerization reactions with the DBU and TEA bases were also investigated computationally. The results of the computational analysis indicate that these neutral nitrogen bases act in a similar fashion as the investigated carboxylate base, because they operate via the same isomerization mechanism, which involves γ -reprotonation as the rate-determining step. For both bases, DBU and TEA, proton transfer to the enolate anion is found to be the highest lying transition state for **14Z** and **14E** thioesters (Figure 4; for details, see the Supporting Information).

The barrier of DBU-assisted isomerization is predicted to be slightly higher than that catalyzed by the pivalate anion (21.5 versus 19.3 kcal/mol for **14Z** and 23.0 versus 21.6 kcal/mol for **14E**). This apparent disagreement with the observed rates is likely due to the simplified carboxylate model that neglects the presence of counterions. Indeed, the reaction rates measured for TMAP and TMGP that differ only in the nature of the

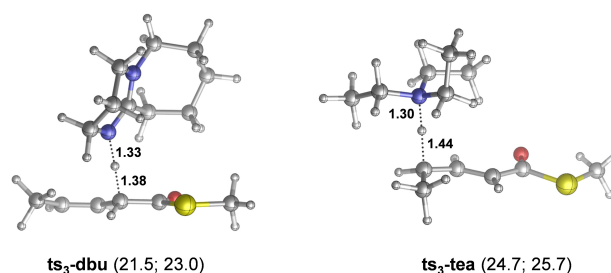


Figure 4. Optimized structures of rate-determining transition states in the isomerization of **14Z** catalyzed by DBU and TEA. Relative stabilities are shown in parentheses (in kcal/mol; with respect to the reactant state **14Z + base**). The second number refers to analogous reaction with **14E** (reference state: **14E + base**). Selected bond distances are given in Å.

counterion show notable variation. Nevertheless, the barrier computed for the weaker TEA base is higher (24.7 and

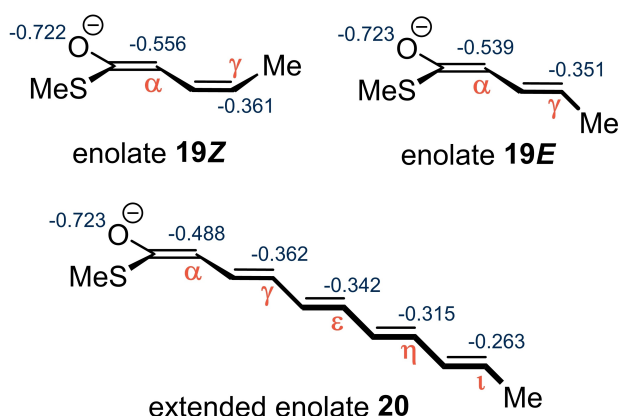


Figure 5. Selected computed carbon atomic NBO charges of enolates **19Z** and **19E** derived from **14Z** and **14E**, respectively, and NBO charges of extended enolate **20**.

25.7 kcal/mol for **14Z** and **14E** thioesters, respectively), which is again consistent with the experimental observations.

The high barrier of the γ -protonation relative to the α -deprotonation mirrors the less negative atomic charge at the γ -carbon compared to the α -carbon (Figure 5). Interestingly, in a longer conjugated enolate such as **20**, the same trend is observed in the series α - γ - ϵ - η - ι , with the ι -carbon bearing the least negative atomic charge (Figure 5). The HOMO coefficients at the carbons follow a similar trend in these enolates (see the Supporting Information). These computational results are in agreement with experimental observations with extended enolates, where generally the α -position shows higher reactivity with electrophiles compared to the γ -position.^[27]

Conclusions

A biomimetic carboxylate-catalyzed isomerization reaction of β,γ -unsaturated thioesters to α,β -unsaturated thioesters proceeds rapidly with TMAP as the base at a rate that is comparable to the rate obtained with DBU. Kinetic isotope effect and computational studies suggest a multistep mechanism where the initial enolization step is not the turnover-limiting step. Instead, the γ -protonation step, where the enolate is reprotonated to generate the product, appears to have the highest barrier. The relatively rapid enolization with carboxylate bases suggests that carboxylate salts in aprotic solvents should be considered as viable non-nucleophilic bases in organic synthesis. TMAP, the base used in this work, is a bench-stable, easily dispensible solid, and it is readily extracted into water upon workup. Research into other applications of carboxylate catalysis is already underway.

Acknowledgements

We acknowledge financial support from the Academy of Finland (projects 297874, 307624, and 322899) and from NKFIH Hungary (grant K-112028).

Conflict of Interest

The authors declare no conflict of interest.

Data Availability Statement

The data that support the findings of this study are available in the supplementary material of this article.

Keywords: base catalysis · carboxylates · enolates · isomerization · kinetic isotope effects · reaction mechanism · thioesters

- [1] Reaxys search (Elsevier). Reaxys reaction search. Enolization of ketone/ester/thioester (2021).
- [2] S. J. Remington, *Curr. Top. Cell. Regul.* **1992**, *33*, 209–229.
- [3] A. J. Mulholland, W. G. Richards, *Proteins Struct. Funct. Bioinf.* **1997**, *27*, 9–25.
- [4] L. Xue, P. Talalay, A. S. Mildvan, *Biochemistry* **1990**, *29*, 7491–7500.
- [5] R. M. Pollack, *Bioorg. Chem.* **2004**, *32*, 341–353.
- [6] R. B. Hamed, E. T. Batchelar, I. J. Clifton, C. J. Schofield, *Cell. Mol. Life Sci.* **2008**, *65*, 2507–2527.
- [7] A. M. Mursula, D. M. F. Van Aalten, J. K. Hiltunen, R. K. Wierenga, *J. Mol. Biol.* **2001**, *309*, 845–853.
- [8] G. U. Onwukwe, M. K. Koski, P. Pihko, W. Schmitz, R. K. Wierenga, *Acta Crystallogr. Sect. D* **2015**, *71*, 2178–2191.
- [9] S. T. Partanen, D. K. Novikov, A. N. Popov, A. M. Mursula, J. K. Hiltunen, R. K. Wierenga, *J. Mol. Biol.* **2004**, *342*, 1197–1208.
- [10] J. A. Gerlt, P. G. Gassman, *J. Am. Chem. Soc.* **1993**, *115*, 11552–11568.
- [11] W. W. Umbreit, R. M. C. Dawson, D. C. Elliott, K. M. Jones, *AIBS Bull.* **1960**, *10*, 45.
- [12] a) J. P. Schwans, F. Sunden, A. Gonzalez, Y. Tsai, D. Herschlag, *J. Am. Chem. Soc.* **2011**, *133*, 20052–20055; b) V. Lamba, F. Yabukarski, M. Pinney, D. Herschlag, *J. Am. Chem. Soc.* **2016**, *138*, 9902–9909.
- [13] D. Uruguchi, Y. Ueki, T. Ooi, *J. Am. Chem. Soc.* **2008**, *130*, 14088–14089.
- [14] For a recent example of the use of stoichiometric carboxylates as bases for the Wittig olefination, see: A. C. Vetter, D. G. Gilheany, K. Nikitin, *Org. Lett.* **2021**, *23*, 1457–1462.
- [15] S.-J. Zhang, W.-X. Hu, *Synth. Commun.* **2010**, *40*, 3093–3100.
- [16] M. E. Muratore, C. A. Holloway, A. W. Pilling, R. I. Storer, G. Trevitt, D. J. Dixon, *J. Am. Chem. Soc.* **2009**, *131*, 10796–10797.
- [17] F. Eckert, I. Leito, I. Kaljurand, A. Kütt, A. Klamt, M. Diedenhofen, *J. Comput. Chem.* **2009**, *30*, 799–810.
- [18] A. Kütt, I. Leito, I. Kaljurand, L. Sooväli, V. M. Vlasov, L. M. Yagupolskii, I. A. Koppel, *J. Org. Chem.* **2006**, *71*, 2829–2838.
- [19] S. Tshepelevitsh, A. Kütt, M. Lökov, I. Kaljurand, J. Saame, A. Heering, P. G. Pliieger, R. Vianello, I. Leito, *Eur. J. Org. Chem.* **2019**, *40*, 6735–6748.
- [20] I. Kaljurand, A. Kütt, L. Sooväli, T. Rodima, V. Mäemets, I. Leito, I. A. Koppel, *J. Org. Chem.* **2005**, *70*, 1019–1028.
- [21] For references, see: DBU: a) K. Kaupmees, K. Trummal, I. Leito, *Croat. Chem. Acta* **2014**, *87*, 385–395; Acetate ion: b) D. Barron, S. Buti, M. Ruiz, J. Barbosa, *Phys. Chem. Chem. Phys.* **1999**, *1*, 295–298.
- [22] T. C. Wilde, G. Blotny, R. M. Pollack, *J. Am. Chem. Soc.* **2008**, *130*, 6577–6585.
- [23] R. M. Pollack, *J. Am. Chem. Soc.* **1991**, *113*, 3838–3842. See also ref 22.
- [24] Y. Wu, R. P. Singh, L. Deng, *J. Am. Chem. Soc.* **2011**, *133*, 12458–12461.
- [25] X. S. Xue, X. Li, A. Yu, C. Yang, C. Song, J.-P. Cheng, *J. Am. Chem. Soc.* **2013**, *135*, 7462–7473.

- [26] The computations were carried out using DFT (M06-2X/Def2-TZVPP/Def2-SVP, SMD solvation model). For details, see the Supporting Information. For simplicity, the counter-cations of the carboxylate bases (TMAP and TMGP) were not included in the modelling, and only the pivalate anion was considered. We are aware that the nature of the counterion influences the reaction rate as shown experimentally, but the analysis of these effects is not straightforward and would require further experimental input. For this reason, their computational analysis was deemed out of scope of the present study.
- [27] a) J. A. Katzenellenbogen, A. L. Crumrine, *J. Am. Chem. Soc.* **1974**, *96*, 5662–5663; b) T. A. Bryson, R. B. Gammill, *Tetrahedron Lett.* **1974**, *15*, 3963–3966; c) I. Fleming, J. Goldhill, I. Paterson, *Tetrahedron Lett.* **1979**, *20*, 3209–3212; d) M. Majewski, G. B. Mpango, M. T. Thomas, A. Wu, V. J. Snieckus, *Org. Chem.* **1981**, *46*, 2029–2045; e) S. Saito, M. Shiozawa, M. Ito, H. Yamamoto, *J. Am. Chem. Soc.* **1998**, *120*, 813–814; f) Y. Terao, T. Satoh, M. Miura, M. Nomura, *Tetrahedron Lett.* **1998**, *39*, 6203–6206; g) S. E. Denmark, G. L. Beutner, *J. Am. Chem. Soc.* **2003**, *125*, 7800–7801; h) S. Kim, C. J. Lim, *Angew. Chem. Int. Ed.* **2004**, *43*, 5378–5380; *Angew. Chem.* **2004**, *116*, 5492–5494; i) J. Y. Lee, S. Kim, *Synlett* **2008**, *1*, 49–54; j) A. M. Hyde, S. L. Buchwald, *Angew. Chem. Int. Ed.* **2008**, *47*, 177–180; *Angew. Chem.* **2008**, *120*, 183–186; k) S. Son, G. C. Fu, *J. Am. Chem. Soc.* **2008**, *130*, 2756–2757; l) S. W. Smith, G. C. Fu, *J. Am. Chem. Soc.* **2009**, *131*, 14231–14233; m) D. S. Huang, J. F. Hartwig, *Angew. Chem. Int. Ed.* **2010**, *49*, 5757–5761, *Angew. Chem.* **2010**, *122*, 5893–5897; *Angew. Chem. Int. Ed.* **2010**, *49*, 5757–5761; n) S. L. Zultanski, G. C. Fu, *J. Am. Chem. Soc.* **2011**, *133*, 15362–15364; o) S. Li, R.-Y. Zhu, K.-J. Xiao, J.-Q. Yu, *Angew. Chem. Int. Ed.* **2016**, *55*, 4317–4321 *Angew. Chem.*, **2016**, *128*, 4389–4393; p) W.-B. Liu, N. Okamoto, E. J. Alexy, A. Y. Hong, K. Tran, B. M. Stoltz, *J. Am. Chem. Soc.* **2016**, *138*, 5234–5237; q) L. Fu, D. M. Guptill, H. M. L. Davies, *J. Am. Chem. Soc.* **2016**, *138*, 5761–5764; r) J. A. Gurak, K. S. Yang, Z. Liu, K. M. L. Engle, *J. Am. Chem. Soc.* **2016**, *138*, 5805–5808; s) X. Chen, X. Liu, J. T. Mohr, *J. Am. Chem. Soc.* **2016**, *138*, 6364–6367.

Manuscript received: April 6, 2022

Accepted manuscript online: May 23, 2022

Version of record online: June 20, 2022